Comparison of Experimental Techniques Used in Lipid Crystallization Studies

A.J. Wright, S.S. Narine, and A.G. Marangoni*

Department of Food Science, University of Guelph, Guelph, Ontario, N1G 2W1, Canada

ABSTRACT: Four methods were used to monitor the crystallization behavior of anhydrous milk fat (AMF), milk fat triacylglycerols (MF-TAG), and MF-TAG plus diacylglycerols (MF-DAG). The crystallization process was monitored by measuring the solid fat content, turbidity, and scattering intensity of the crystallizing material, as well as by imaging using polarized light microscopy combined with digital image processing. In general, induction times followed the order MF-DAG > AMF > MF-TAG for all techniques. However, the absolute value for the induction times differed substantially; on average 3 min by microscopy, 7 min by light-scattering spectroscopy, 13 min by turbidimetry, and 25 min by pulsed nuclear magnetic resonance. Microscopic imaging coupled to image processing proved to be the most sensitive method, suitable for the study of early events in the crystallization of fats.

Paper no. J9562 in *JAOCS 77*, 1239–1242 (December 2000).

KEY WORDS: Crystallization, image analysis, induction times, pNMR, polarized light microscopy, turbidimetry.

Crystallization of fats is considered to encompass two distinct events, nucleation and crystal growth. While a stable nucleus must be formed before crystal growth can occur, these events are not mutually exclusive. Nucleation may take place while crystals grow on existing nuclei (1). In our investigations of the effects of minor components on milk fat crystallization, it became clear that minor components delayed crystallization of milk fat triacylglycerols (2). However, it was difficult to discern whether the effects were at the nucleation or crystal growth level. Distinguishing between nucleation and crystal growth constitutes a major challenge in lipid crystallization studies.

The shape of a crystallization curve can provide some insight into the mode of crystal growth (3). However, the nucleation step is more elusive because the methods typically used in these studies are relatively insensitive. Pulsed nuclear magnetic resonance (pNMR), which measures solid fat content (SFC), and light-scattering techniques, which measure absorbance or transmittance of light, are commonly used to monitor lipid crystallization. Anyone familiar with the pNMR method knows that, at times, small amounts of crystals are visible in the melt before any solids are detected. Clearly, at this stage, well beyond the induction time for nucleation, the pNMR signal is measuring crystal growth. Turbidimetry, while more sensitive than pNMR, e.g., shorter induction times are obtained, also has its limitations. In fact, a very strong correlation was found between induction times by pNMR and turbidimetry for the three fat systems used in the minor components study, suggesting that increases in turbidity are also due to mass deposition of crystals and not only nucleation (2).

It would be beneficial to have a convenient way of unambiguously determining nucleation induction times when seeking to understand the effects of varying composition and processing conditions on nucleation, and it is essential if the induction times are used in mathematical models such as the Fisher-Turnbull equation (4). In the Fisher-Turnbull model, activation free energies of nucleation are calculated from nucleation induction times. The usual assumption is that the experimental technique used to determine the induction time provides an accurate measure of the nucleation rate.

Induction times for this purpose have been determined using light-scattering techniques (5). Herrera *et al*. (6) used a modified laser-polarized light turbidimetric approach to obtain induction times, the details of which were described by Herrera (7). Polarized light microscopy (PLM) has also been used to visually observe the onset of nucleation (6,8). Similarily, nucleation and growth rates in palm oil were determined microscopically using polarized light in conjunction with a counting cell and graduated ocular (9). A similar method was automated using PLM in conjunction with a CdS photo sensor. Instead of observing the sample visually, the sensor monitored the transmission of light through the crystallizing sample on a microscope slide (10). This is a very sensitive approach; however, the specialized equipment required is not commonly available. In this study, induction times determined by pNMR and turbidity measurements are compared to those determined using PLM in conjunction with image analysis. This research was carried out in the context of our milk fat minor components study (2).

MATERIALS AND METHODS

Minor components (nontriacylglycerol species) were removed from anhydrous milk fat (AMF) to obtain purified milk fat triacylglycerols (MF-TAG) by column chromatography using Florisil as the stationary phase (2). As previously described,

*To whom correspondence should be addressed.
E-mail: amarango@uoguelph.ca

the crystallization behavior of the original AMF, the MF-TAG, and MF-TAG to which 0.1% milk fat diacylglycerol was added (MF-DAG) was studied by pNMR and turbidimetry (2). Although crystallization was studied between 5.0 and 27.5°C, we will concentrate only on data collected at 22.5°C.

In addition, crystallization was followed using polarized light microscopy at 22.5°C. AMF, MF-TAG, and MF-DAG were preheated to 80°C for 10 min before a drop of each was placed on a preheated (80°C) glass microscope slide and covered with a preheated (80°C) glass coverslip. The samples were imaged with a Zeiss (Oberkochen, Germany) polarized light microscope using a 10 × objective and equipped with a CCD Video Camera (Sony, Tokyo, Japan). Temperature of the slide was maintained at 22.5°C. Crystallization was followed by capturing an image every 15 s for 30 min. The images were processed using Image Tool (The University of Texas Health Science Center, San Antonio, TX). A background subtraction was performed initially by subtracting the initial image (time = 0 s) for each of AMF, MF-TAG, and MF-DAG from every other image in the respective crystallization run. The images were manually thresholded, using the same value for every image in each of AMF, MF-TAG, and MF-DAG. The threshold level was that which was found to most accurately reflect the original greyscale images. Once the images were thresholded, the relative amounts of black and white pixels in each image were determined. The amount of black (representing crystal mass) was plotted as a function of crystallization time.

For the light-scattering studies, a phase transition analyzer (Phase Technology, Richmond, British Columbia, Canada) was used. One hundred fifty microliters of sample, preheated to 80°C for 30 min, was pipetted into the sample container of the analyzer, which was preheated and maintained at 75°C using a thermoelectric cooler. Thereafter, the sample was rapidly cooled from 75 to 22.5°C at a controlled rate of 50°C/min. When the sample reached 22.5°C, it was held at this temperature and crystallization was continuously monitored using an optical scattering approach. In this setup, a beam of light impinges on the sample from above. A matrix of optical sensors, in tandem with a lens system, is also placed perpendicularly above the sample. When crystals start to appear in the sample, the incident beam is scattered by the solid–liquid phase boundaries and scattered light impinges *via* the lens onto the detectors. As more and more crystal mass develops, the signal output increases and is automatically recorded.

Results for pNMR, turbidity, light scattering, and image analysis were normalized by dividing each value by the maximum crystallization value and the resulting fractional crystallization values compared. Induction times were determined by extrapolating the linear portion of the crystallization curves to the time axis. For the pNMR, turbidity, and microscopy experiments induction times were taken from the time when the sample was immersed at 22.5°C. For the light scattering experiments, timing began when the samples reached 22.5°C. However, differences in cooling rates between the four methods could also influence crystallization.

RESULTS AND DISCUSSION

Figure 1 shows thresholded polarized light micrographs of MF-TAG at various crystallization times at 22.5°C. Crystallization curves for AMF, MF-TAG, and MF-DAG by pNMR, turbidity, and PLM-image analysis are shown in Figure 2. MF-TAG crystallized first, followed by AMF and MF-DAG. MF-DAG had the longest induction times as determined by pNMR, while by turbidimetry and microscopy, AMF had the longest induction time. Although the relative trends were similar, Figure 2 shows that there were large differences in the absolute value of onset times of crystallization between the three methods. Crystallization curves for AMF, MF-TAG, and MF-DAG obtained from measurements of light-scattering intensities are shown in Figure 3. In this case, MF-TAG crystallized first and AMF had the longest induction time. The two curves for MF-TAG demonstrate the technique's reproducibility. The induction times for the crystallization curves are reported in Table 1.

Table 1 shows that the induction times determined by pNMR were the longest, while those determined by the image analysis technique were the shortest. Therefore, with the image analysis approach we were able to detect some early crystallization events beyond the sensitivity of the other methods. The higher sensitivity demonstrated allowed for the detection of early crystallization events, possibly in the vicinity of the true nucleation events.

A simple calculation can highlight the reason why the microscopic technique is more sensitive than pNMR and turbidity measurements. Solids in a 30-mg fat sample (ρ = 0.90 g/cm^3) with an SFC of 0.1% (w/w) occupy a volume of $3.33 \cdot 10^{-11}$ m^3. The volume of a spherical nucleus of 0.5 μm diameter is $6.54 \cdot 10^{-20}$ m^3. If all of this solid mass corresponded to nuclei, $5.1 \cdot 10^8$ nuclei would be present in this sample. An

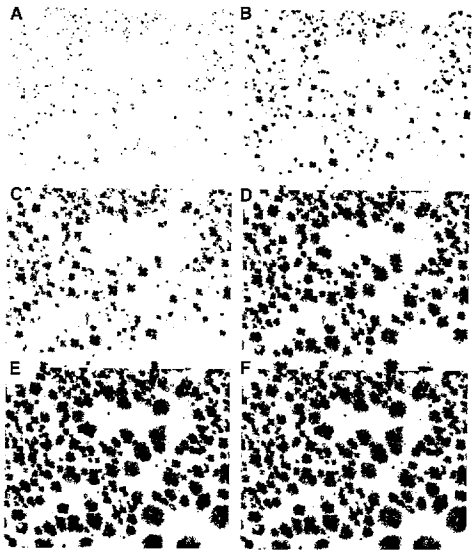

FIG. 1. Thresholded polarized light microscope images of milk fat triacylglycerol (MF-TAG) at various crystallization times at 22.5°C: (A) 1 min, (B) 3 min, (C) 5 min, (D) 10 min, (E) 20 min, (F) 28min.

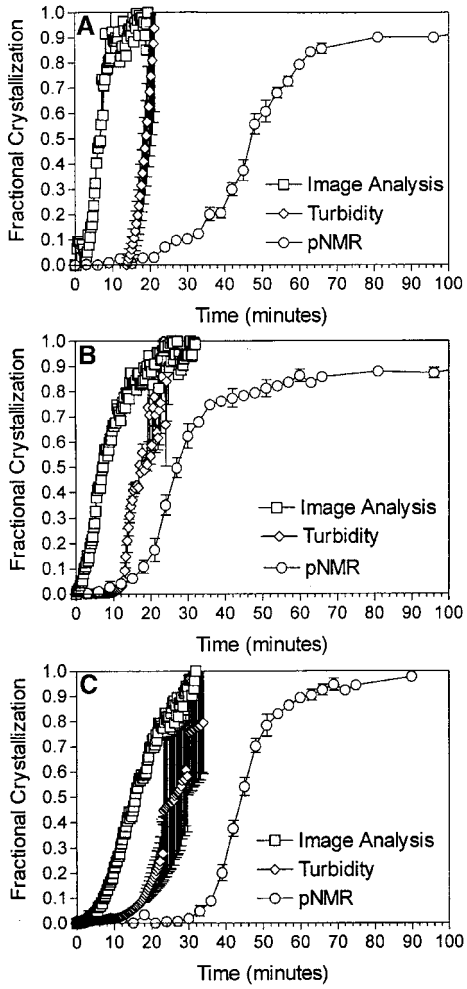

FIG. 2. Fractional crystallization of anhydrous milk fat (AMF) (A), MF-TAG (B), and MF-TAG plus diacylglycerol (MF-DAG) (C) determined by pulsed nuclear magnetic resonance (pNMR) measurements of solid fat content, turbidity measurements, and polarized light microscopy coupled to image analysis at 22.5°C. Symbols in (A), (B), and (C) represent the average and standard errors of three replicates. See Figure 1 for other abbreviation.

SFC of 0.1% is below the detection threshold of a pNMR machine. Two obvious conclusions can be drawn from these calculations. Even at 0.1% SFC, the solids present in the sample cannot solely correspond to nuclei, since their number would

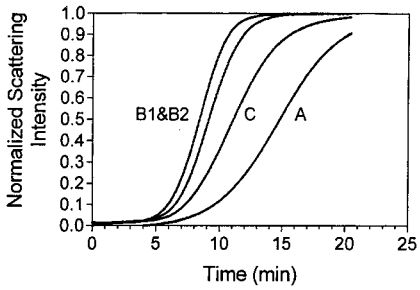

FIG. 3. Fractional crystallization of AMF (A), MF-TAG (B1 and B2), and MF-DAG (C) determined by light-scattering spectroscopy. See Figures 1 and 2 for abbreviations.

be too great. Microscopic observation of a typical 30-mg sample of crystallizing fat (0.1% SFC) should convince any skeptic that $5.1 \cdot 10^8$ nuclei cannot possibly be present. This suggests that by the time that SFC values reach 0.5–1.0%, a typical detectable level in a pNMR machine, significant amounts of crystal growth must have necessarily taken place. Therefore, an induction time of crystallization determined by pNMR does not correspond to the induction time for nucleation.

Turbidimetry is a more sensitive technique for the study of the early stages of a crystallization process than pNMR (2). Turbidimetry relies on the scattering of light by newly formed or growing crystals. Scattering produces two effects on the transmitted beam: (i) a loss of transmitted intensity due to scattering of the radiation at angles other than 0° (turbidity), and (ii) an apparent change in velocity of the transmitted beam (refraction). A change in the velocity of the transmitted beam due to scattering results in a change in the refractive index of the medium, which will itself affect the measured turbidity.

The ratio of the intensity of the light beam after its passage through a sample (I) over the intensity of the incident light beam (I_o) is related to the concentration of scattering material by Beer's law:

$$\frac{I}{I_o} = e^{-\tau l c} \qquad [1]$$

where τ is a turbidity parameter (m^2/kg) similar to an extinction coefficient, l is the sample thickness (m), and c is the concentration of scattering material (kg/m^3). The signal measured in a common spectrophotometer is the absorbance (or transmittance) due to scattering, $A_s = -\ln(I/I_o)$. Hence,

TABLE 1
Induction Times for AMF, MF-TAG, and MF-DAG Determined by pNMR, Turbidity, Light-Scattering Intensity Measurements, and Polarized Light Microscopy Coupled to Image Analysis[a]

	pNMR (min)	Turbidity (min)	Light scattering (min)	Microscopy (min)
AMF	28.2 (4.2%)	14.9 (8.4%)	9.0 (0.5%)	3.0 (3.8%)
MF-TAG	14.7 (6.2%)	12.3 (11.8%)	6.3 (1.1%)	1.5 (3.0%)
MF-DAG	33.3 (4.9%)	12.9 (11.0%)	7.0 (0.7%)	5.3 (1.8%)

[a]Values represent averages and percentage standard errors. Abbreviations: AMF, anhydrous milk fat; MF-TAG, milk fat triacylglycerols; MF-DAG, MF-TAG plus diacylglycerols; pNMR, pulsed nuclear magnetic resonance.

$$A_s = \tau l c \quad [2]$$

The turbidity parameter (τ) is related to the Rayleigh ratio at 90° (R_{90}) by (11):

$$\tau = \frac{16\pi}{3} R_{90} \quad [3]$$

The Rayleigh ratio for a solution containing N scattering centers per unit volume is given by (11):

$$R_{90} = \frac{8\pi^4 \alpha^2}{\lambda^4} N \quad [4]$$

where α is the molecular polarizability of the system, which is a function of the shape of the electron cloud and the frequency of the applied radiation, and λ is the wavelength of the applied radiation. Hence, τ is proportional to the number of scattering centers per unit volume.

The molecular polarizability is related to the difference in refractive indices of the pure solvent and the solution/suspension by the relationship (11):

$$\alpha = \frac{n_s^2 - n_0^2}{4\pi N} \quad [5]$$

where n_s corresponds to the refractive index of the solution/suspension, and n_o corresponds to the refractive index of the pure solvent. Substituting Equations 3, 4, and 5 into Equation 2, we obtain the following expression for A_s:

$$A_s = \frac{8\pi^3 l (n_s^2 - n_o^2)^2}{3\lambda^4} \left(\frac{c}{N}\right) \quad [6]$$

The absorbance of light due to scattering is proportional to the ratio of the concentration of crystallized material to the number of scattering centers per unit volume. Hence, in the vicinity of a nucleation event, a small amount of mass is distributed among a large number of nuclei, resulting in a small value of c/N. This, in turn, results in a small value of A_s, which implies an inherent physical limitation in the ability of the technique to detect nucleation events. The reader should keep in mind that the simplified treatment shown above applies only to dilute solutions/suspensions, where scattering centers are small relative to the wavelength of the incident light.

Another complicating factor in the measurement of turbidity is the absorption of light by colored materials in the sample, thus reducing the intensity of the measured signal and therefore the sensitivity of the technique. Impurities such as dust can contribute to high background scattering, reducing the signal-to-noise ratio. If the light used is not monochromatic, such as in case of diode-array spectrophotometers, a distribution of scattering events at different wavelengths will take place. Signal intensity can be lost due to the presence of slits on the detector side of the spectrophotometer, which cut out much of the transmitted beam. As well, only a small volume of the element is sampled during measurement, roughly the diameter of the light beam. All of these factors result in a decrease in the sensitivity of the technique, and its ability to detect nucleation events.

Light-scattering spectroscopy proved to be a more sensitive method than turbidimetry. In this method, the intensity of scattered light, rather than the attenuation of the signal intensity (I/I_o), is measured. The particular geometry of the sample cell and positioning of the detectors also maximize the collection of the scattered light. This technique proved to be very convenient, user-friendly, and reproducible.

PLM has inherent advantages over turbidimetry. The PLM technique exploits the difference in refractive index of a beam of incident light polarized in two perpendicular directions. This phenomenon is known as birefringence. Anisotropic materials, such as a fat crystal, will display birefringence. Since fat crystals are birefringent, they will appear as sharp bright objects in a non-birefringent, and therefore dark, background. The use of polarizers set at 90° removes most of the non-birefringent background signal (colored melt and scattering impurities), thereby considerably increasing the signal-to-noise ratio. Also, since all of the transmitted light beam in the field of view is collected by the lenses and focused on the camera, signal intensity and therefore sensitivity are increased.

ACKNOWLEDGEMENT

The authors would like to acknowledge Dr. Gordon Chiu from Phase Technology (Richmond, British Columbia, Canada) for the light-scattering analysis.

REFERENCES

1. Sato, K., Crystallization Phenomena in Fats and Lipids, *J. Dispersion Sci. Technol. 10*:363–392 (1989).
2. Wright, A.J., R.W. Hartel, S.S. Narine, and A.G. Marangoni, The Effect of Minor Components on Milk Fat Crystallization, *J. Am. Oil Chem. Soc. 77*, 463–475 (2000).
3. Sharples, A., *Introduction to Polymer Crystallization*, Edward Arnold Ltd., London, 1966, pp. 44–59.
4. Strickland-Constable, R.F., Nucleation of Solids, in *Kinetics and Mechanism of Crystallization*, Academic Press, London, 1968, pp. 74–129.
5. Herrera, M.L., M. de Leon Gatti, and R.W. Hartel, A Kinetic Analysis of Crystallization of a Milk Fat Model System, *Food. Res. Int. 32*:289–298 (1999).
6. Herrera, M.L., C. Falabella, M. Melgarejo, and M.C. Añón, Isothermal Crystallization of Hydrogenated Sunflower Oil: I—Nucleation, *J. Am. Oil Chem. Soc. 75*:1273–1280 (1998).
7. Herrera, M.L., Crystallization Behavior of Hydrogenated Sunflowerseed Oil: Kinetics and Polymorphism, *Ibid. 71*:1255–1260 (1994).
8. Ng, W.L. A Study of the Kinetics of Nucleation in a Palm Oil Melt, *Ibid. 67*:879–882 (1990).
9. van Putte, K.P.A.M., and B.H. Bakker, Crystallization Kinetics of Palm Oil, *Ibid. 64*:1138–1143 (1987).
10. Koyano, T., I. Hachiya, T. Arishima, K. Sato, and N. Sagi, Polymorphism of POP and SOS. II. Kinetics of Melt Crystallization, *Ibid. 66*:675–679 (1989).
11. Campbell, I.D., and R.A. Dwek, Scattering, in *Biological Spectroscopy*, The Benjamin Cummings Publishing Company, Inc., Menlo Park, 1984, pp. 217–238.

[Received March 17, 2000; accepted August 5, 2000]